

Test on cyclic creep behavior of mucky clay in Shanghai under step cyclic loading

Yi-Qun Tang · Jie Zhou · Sha Liu ·

Ping Yang · Jian-Xiu Wang

Received: 12 May 2009 / Accepted: 12 August 2010 / Published online: 26 August 2010
© Springer-Verlag 2010

Abstract Based on the cyclic triaxial test under step loading, the variation of cyclic creep and pore water pressure with increase in cyclic stress ratio (CSR) and load cycle of mucky clay in Shanghai were analyzed. The results show that there are two threshold values of stability cyclic stress ratio and failure cyclic stress ratio during the step loading which divide the development of cyclic creep strain into gradual stability stage, rapid growth stage and instantaneous failure stage. When the stress level is less than the failure cyclic stress ratio, the recoverable elastic strain is nearly linear with CSR. The cyclic creep properties of mucky clay are obviously influenced by the loading frequency under the same stress level.

Keywords Mucky clay · Cyclic creep · Pore water pressure · Step cyclic loading

Introduction

Induced by the soil viscous property, creep phenomena of clay are of great influence to the soil consolidation, slope stability and ground bearing capacity, especially when

long-term cyclic loadings like traffic or wave loadings are conducted. According to the field investigation in Saga Airport, the subsequent settlement caused by traffic loading has reached 15 cm (Miura et al. 1995). More serious problems have occurred in Shanghai where most are soft clay areas. The tunnel settlement along axial line in some part of Shanghai subways has exceeded 20 cm, which not only affects the normal subway operating, but also leads to the old buildings' cracking along subway lines (Wang and Liu 2000). It is of important engineering significance to investigate the creep characteristics of clay under long-term cyclic loading.

Since early 1960s there are many researches on the creep behaviors of clay under cyclic loading. Seed and Chan (1961) investigated the low embankment deformation under reciprocating traffic loading. In order to construct the gravity offshore platform, Andersen et al. (1980) conducted comprehensive research on Drammen clay characteristics under wave loading. Considering the element of pore water pressure dissipation, Hyodo et al. (1992) studied the pore water pressure and residual settlement of saturated soft clay in the subgrade under traffic loading. A model for predicting the cyclic behavior of soft clay was presented by Zhou and Tu (1996), while the one-dimensional sedimentation of clay under long-term cyclic loading was estimated by Jun and Chen (2001) from China. Moreover, in the last decade the frequent occurrence of subway accidents all over the world resulted that more and more attentions have been paid to various soil behaviors under the cyclic reciprocating loading. Chai and Miura (2002) presented a method for predicting the traffic-load-induce settlement of road on soft subsoil with a low embankment. Moses et al. (2003) carried out a series of cyclic triaxial shear tests to study the influence of the strain effect and load cycles on the undrained shear strength of

Y.-Q. Tang (✉) · P. Yang · J.-X. Wang
Key Laboratory of Geotechnical and Underground Engineering
of Ministry of Education, Tongji University,
Shanghai 200092, People's Republic of China
e-mail: tangyiqun2@tongji.edu.cn

P. Yang
e-mail: csuyangp@163.com

Y.-Q. Tang · J. Zhou · S. Liu · P. Yang · J.-X. Wang
Department of Geotechnical Engineering, Tongji University,
Shanghai 200092, People's Republic of China
e-mail: zoujer@hotmail.com

cemented marine clay. Tang et al. (2003) conducted the dynamic triaxial test of silt soils around the tunnel in Nanjing under subway train loading, presented the variations of critical dynamic stress ratio and dynamic strain with time. Subsequently the dynamic strength behavior was also studied and several significant conclusions were obtained (Tang et al. 2004). Yilmaz et al. (2004) focused on the deformation behavior and undrained cyclic shear to consider of the severity of foundation displacements. Boulanger and Idriss (2007) gave a kind of method to evaluation the potential for cyclic softening. Guan et al. (2009) estimated the rheological parameter for the prediction of long-term deformations in tunneling. However, most of these researches are focused on the residual deformation prediction in the long-term cyclic loading, and little attention was paid to the essential characteristic and variation of clayey creep. Hence, in order to avoid or control the engineering geological disaster caused by subway operation, it is indispensable to make experimental researches on the essential properties of clayey creep under cyclic loading.

By means of cyclic triaxial test under step loading conducted on undisturbed soil samples from the fourth soil stratum in Shanghai, the paper studies the variation of cyclic creep and pore water pressure of mucky clay with increase in cyclic stress ratio and number of loading cycles.

Test apparatus and samples

The dynamic cyclic triaxial test system, Geotechnical Digital Systems (GDS), which was produced by GDS instruments Ltd in Britain, was utilized during the whole test. Composed of triaxial pressure chamber, confining pressure controller, back pressure controller, axial loading driver, measuring apparatus, data collector and computer, GDS can meet the needs of sacton and consolidation test, standard and advanced triaxial test, stress path test, permeability test and dynamic triaxial test, respectively, using different test software modules.

Test samples used in the study were mucky clay drilled from the fourth soil stratum in Shanghai with the depth of 13.5 m near Jingan Temple Station of NO. 2 line of Shanghai Metro. With the thickness of 10 m, the mucky clay stratum with mica and shell debris and thin silt has high natural moisture content, large void ratio, high

compressibility, low strength and medium–high sensitivity. Some physical index properties were presented in Table 1.

Test control parameter and procedures

Axial sinusoidal cyclic loading was applied on the samples under step loading during the tests. The field monitoring was carried out by Zhao (2005) from Jingan Temple Station to Jiangsu Road Station of NO. 2 line of Shanghai Metro and the results showed that the response frequencies of mucky clay around subway tunnels focus on high frequency section of 2.4–2.6 Hz and low frequency section of 0.4–0.6 Hz. Consequently, the cyclic loading frequencies in the tests were set to be 0.5 and 2.5 Hz for comparison. All the test parameters are summarized in Table 2.

Test procedures are as follows: (1) The sampler was cut into a cylindrical specimen of 38 mm diameter and 80 mm height, which was fixed into the triaxial pressure chamber before the test. (2) Back pressure was applied on the sample utilizing the Sacton software module for more than 120 min to make the sample fully saturated. The pore water pressure coefficient B-value was measured to confirm the saturation until it reaches to 0.98. (3) To simulate the field stress condition, sample was consolidated utilizing Advanced Triaxial Test software module under the condition that the value of lateral pressure coefficient K_0 was about 0.7, which lasted for more than 24 h till axial strain rate was less than 0.05%/h. (4) Cyclic triaxial test was conducted continuously on the sample with Advanced Triaxial Test software module under step loading, in which the initial cyclic stress amplitude was 10 kPa, the periodical amplitude increment was 5 kPa and the number of loading cycles in each step stage was 2,000 times. The whole step loading process was shown in Fig. 1.

Test results and analysis

Composition of cyclic creep

Test results show that the soil samples have very similar creep behaviors under cyclic loading in each step stage. Take a typical stage for example, which is the cyclic stress amplitude of 10 kPa, the loading cycles of 2,000 times and the cyclic loading frequency of 0.5 Hz. The cyclic loading during this stage is described in Fig. 2.

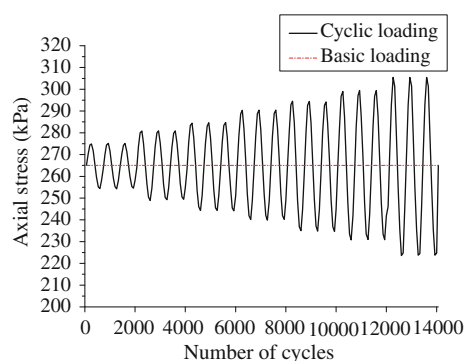
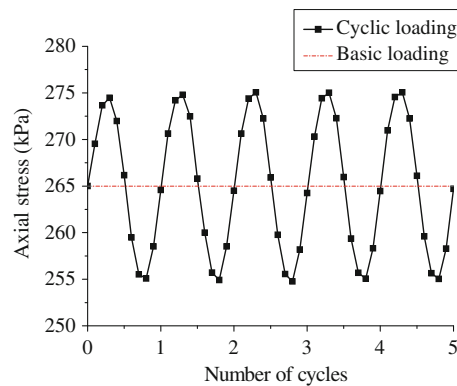
Figure 3 shows the cyclic creep curve (Fig. 3a), variational pore water pressure curve (Fig. 3b) and deviator stress–strain curves (Fig. 3c) of the sample during the first five cycles in the stage mentioned above. In each cycle, ten data points were collected by the computer automatically. It can be observed in Fig. 3a that the creep curve gradually

Table 1 The physical index properties of samples

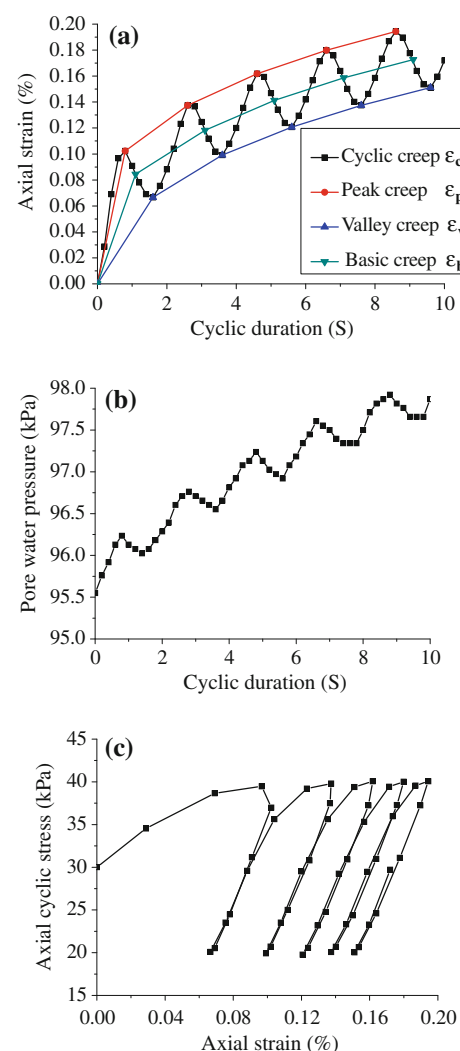
Soil strata label	Natural moisture content (%)	Natural unit weight (kN/m)	Liquid limit (%)	Plastic limit (%)
④	50.2	16.6	43.4	23.2

Table 2 Control parameters of cyclic triaxial tests

Test plan	Vibration waveform	Basic pressure (kPa)	Cell pressure (kPa)	Back pressure (kPa)	Stepped stress amplitude (kPa)	Loading frequency (Hz)
A	Sinusoidal	265	195	100	5	0.5
B	Sinusoidal	265	195	100	5	2.5

**Fig. 1** Step cyclic loading during the cyclic triaxial test**Fig. 2** Sinusoidal cyclic loading during the typical stage

drifts up in an approximately sinusoidal waveform. After linking each peak point and valley point of strain in each loading cycle, respectively, two new curves were obtained, which are defined as peak creep curve (ε_p) and valley creep curve (ε_v). Then based on the test data and the formula $\varepsilon_b = (\varepsilon_p + \varepsilon_v)/2$, basic creep curve (ε_b) is obtained. Just as it is seen in Fig. 3a, these three curves not only have the same variation trend of strain increasing with the growth rate decaying, but also indicate that the total cyclic creep process of mucky clay in Shanghai nearly changes in a certain amplitude on the basis of basic creep (ε_b). On one hand, the value of recoverable elastic strain (ε_e) during the test can be defined as $\varepsilon_e = (\varepsilon_p - \varepsilon_v)/2$, then $\varepsilon_p = \varepsilon_b + \varepsilon_e$ and $\varepsilon_v = \varepsilon_b - \varepsilon_e$. This recoverable elastic strain actually shows soil's elastic property. On the other hand, the incremental tendency of basic creep implies that, there is an amount of irreversible plastic strain accumulation in soil samples during each loading cycle, and the accumulating

**Fig. 3** Creep/Pw-time curves and stress-strain curve in initial five cyclic periodicities. **a** Cyclic creep, **b** pore water pressure (c) deviator stress-strain curves

rate of plastic strain has a decreasing trend. The nature of basic creep is the accumulated plastic strain, which validates soil's plastic property. Hence, it can be concluded that the total cyclic creep process of mucky clay in Shanghai is composed of relatively constant recoverable elastic strain and progressively attenuating accumulated plastic strain.

The variation curve of pore water pressure in the soil sample is depicted in Fig. 3b. With the number of cycles increasing, the curve drifts up as the time increases in an

irregular sinusoidal waveform, in which there is a similarity with the creep curve behaviors discussed above. The typical deviator stress–strain curve in initial cyclic loading duration is described in Fig. 3c. It can be distinctly seen that the mucky clay has great hysteresis property, as the hysteresis hoops both move right and become dense gradually with the cycles increasing, which implies again that, an amount of irreversible plastic strain accumulated in soil samples during each loading cycle, and the accumulating rate rapidly decreases, with the final irreversible strain converging to a certain finite value.

The characteristics of the soil sample in the final five cycles of the typical stage are described in Fig. 4, including the corresponding cyclic creep curves (Fig. 4a), pore water pressure curve (Fig. 4b) and deviator stress–strain curves (Fig. 4c). The three creep curves in Fig. 4a change to be nearly parallel and horizontal, reflecting that the accumulating rate of plastic strain in the soil sample decreased

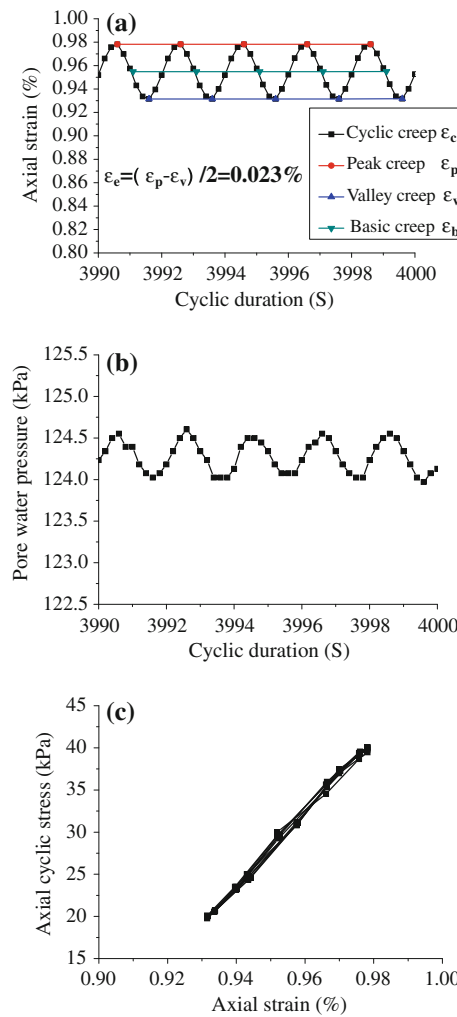


Fig. 4 Creep/Pw–time curves and stress–strain curve in final five cyclic periodicities. **a** cyclic creep, **b** pore water pressure, **c** deviator stress–strain curves

nearly to be zero and the accumulated soil deformation tended to a constant. According to the formula $\varepsilon_e = (\varepsilon_p - \varepsilon_v)/2$, it can be calculated with the datum from Fig. 4a that, the recoverable elastic strain in the typical stage finally converges to be stable value 0.023%. Similarly, the pore water pressure in the final 5 cycles is going to be stable in Fig. 4b. Figure 4c shows a superposition of the deviator stress–strain curve. It proves again that with the time of loading cycles increasing, the soil grains gradually tend to be dense and plastic deformation tends to mitigation. Consequently, the hysteresis hoops are going to be overlapped, but not move to the right.

Recoverable elastic strain in each stage of step cyclic loading

The same analytical method discussed above in the typical stage was applied on each step loading, in which different cyclic amplitude was conducted on test soil samples, to calculate all the recoverable elastic strain values. Results show that, the recoverable elastic strain of each stage is different due to different cyclic stress amplitudes and loading frequencies.

Figure 5 plots the relation curves of recoverable elastic strain with different cyclic stress amplitudes, including Fig. 5a, b under loading frequencies of 0.5 and 2.5 Hz during the whole cyclic triaxial test, respectively. It can be obviously seen that recoverable elastic strain becomes

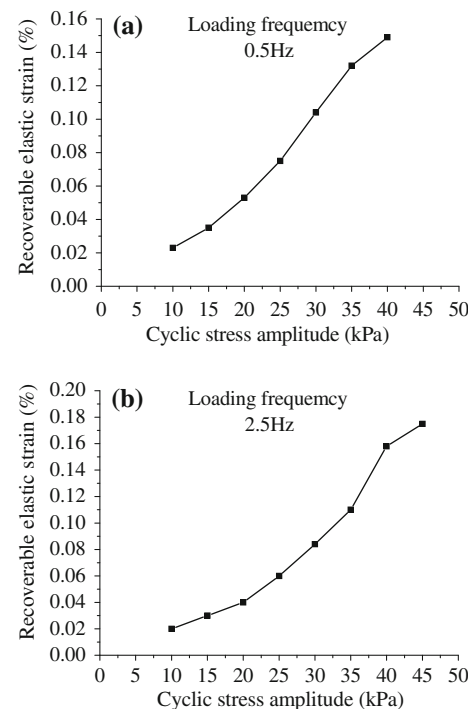


Fig. 5 Recoverable elastic strain versus cyclic stress amplitude curves with loading frequency. **a** $f = 0.5$ Hz, **b** $f = 2.5$ Hz

larger with the cyclic stress amplitude increasing. Additionally, threshold stress amplitude of cyclic loading was discovered during the step loading process. When exceeding this threshold value, the cyclic creep of soil sample increased sharply and the sample instantaneously collapsed. The growth rate of recoverable elastic strain changes from increasing to decreasing. Just as Fig. 5 shows, there is a turning point of the incremental trend in each curve. If cyclic stress ratio of the soil sample is defined by the formula $CSR = \frac{q_{cyc}}{2\sigma} = \frac{3q_{cyc}}{2(\sigma_1 + \sigma_2 + \sigma_3)}$, the corresponding cyclic stress amplitude can be defined as failure cyclic stress ratio. Figure 5 also implies that the loading frequency has an influence on the value of failure cyclic stress ratio. The threshold stress amplitude in Fig. 5a, b are 35 and 40 kPa, respectively, that is, the failure cyclic stress ratio under loading frequency of 0.5 and 2.5 Hz are 0.14 and 0.16. These values indicate that, with the same stress level in the frequency section of 0.5–2.5 Hz, the higher the loading frequency applied, the greater the failure cyclic stress ratio of mucky clay in Shanghai.

The two graphs in Fig. 6 obviously show that there is a linear relation between the recoverable elastic strain and the cyclic stress ratio, when the stress level is below failure cyclic stress ratio. This conclusion is basically consistent with that of Zhu et al. (2005). Compared with the two formulas by linear fitting in Fig. 6, it can also be detected

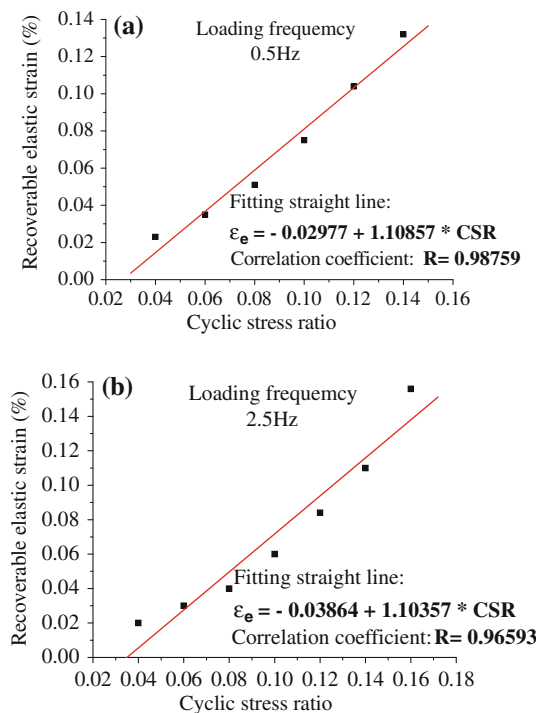


Fig. 6 Fitting lines between recoverable elastic strain and cyclic stress ratio with loading frequency

that the loading frequency has no significant influence on this linear relationship.

The relation between loading frequency and recoverable elastic strain under different cyclic stress ratios are depicted in Fig. 7, from which conclusions can be drawn that the value of recoverable elastic strain is influenced by loading frequency. Under the same stress level, lower frequency load resulted in a larger recoverable elastic strain. And as it is seen in the figure, the slope of lines change from nearly vertical to sloping and the gradients are greater and greater with the stress level increasing.

Variation of accumulated plastic strain and residual pore water pressure in the whole test

Test results show that the pore water pressure in the soil sample has a similar variation with its cyclic creep. Consequently, based on the experiment data and the calculation formula discussed above, the basic creep curve and the basic pore water pressure curve can be drawn. As a matter of fact, these two curves describe the variation of the accumulated plastic strain and residual pore water pressure in the soil samples, respectively.

Figure 8 reflects the accumulation of plastic strain at loading frequency of 0.5 Hz in Fig. 8a and 2.5 Hz in Fig. 8b, respectively. Both the curves change from nearly horizontal to sloping and at last come to almost vertical. It implies that there are two threshold cyclic stress ratio values under step cyclic loading, thus dividing the variation of the accumulated plastic strain into gradual stabilization stage, rapid growth stage and instantaneous failure stage. The first threshold value can be defined as stability cyclic stress ratio, while the second one can be defined as the failure cyclic stress ratio discussed above. Additionally, it can be seen from the figures that values of the two CSRs are approximately 0.08 and 0.14 with the frequency of 0.5 Hz, while 0.08 and 0.16 with the frequency of 2.5 Hz.

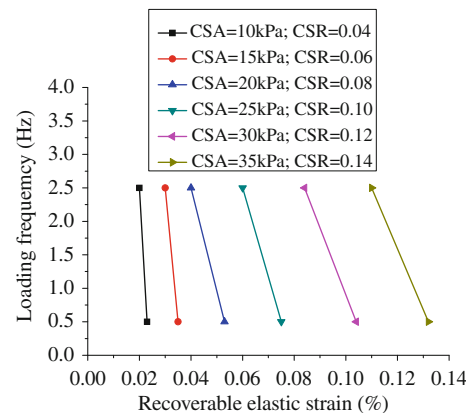


Fig. 7 Loading frequency versus recoverable elastic strain under different cyclic stress ratios

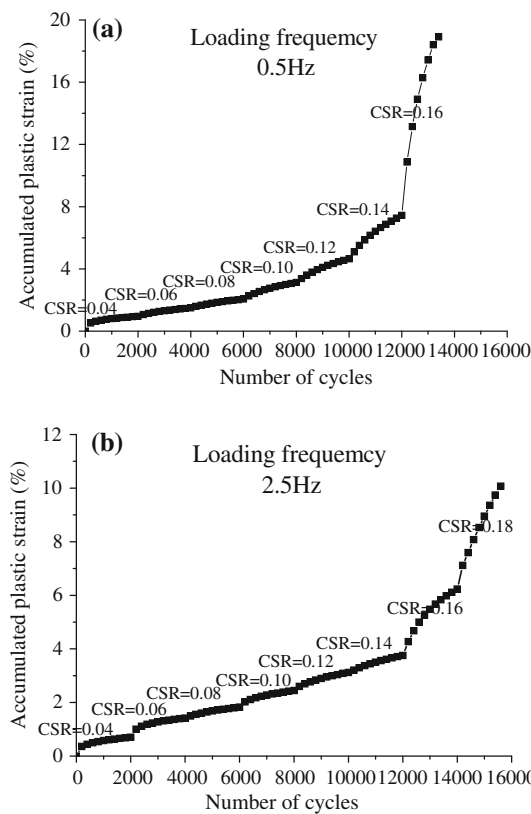


Fig. 8 Accumulated plastic strain versus number of cycles with loading frequency

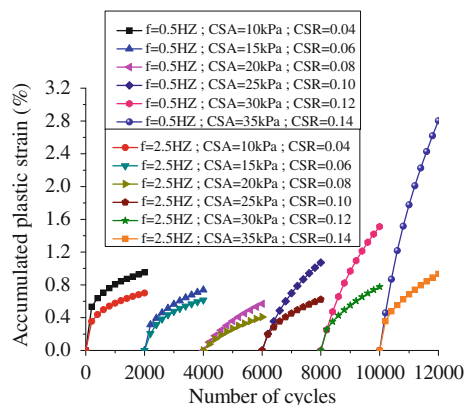


Fig. 9 Comparative curves of accumulated plastic strains with different loading frequencies

It reflects that the frequency of cyclic loading has no significant influence on the soil's stability cyclic stress ratio, while has an influence on the soil's failure cyclic stress ratio, that is, failure cyclic stress ratio gets greater under cyclic loading with higher frequency.

The comparison of accumulated plastic strain under each step loading and different loading frequencies are depicted in Fig. 9. Six groups of contrast curves show that under the same loading level, the accumulated plastic

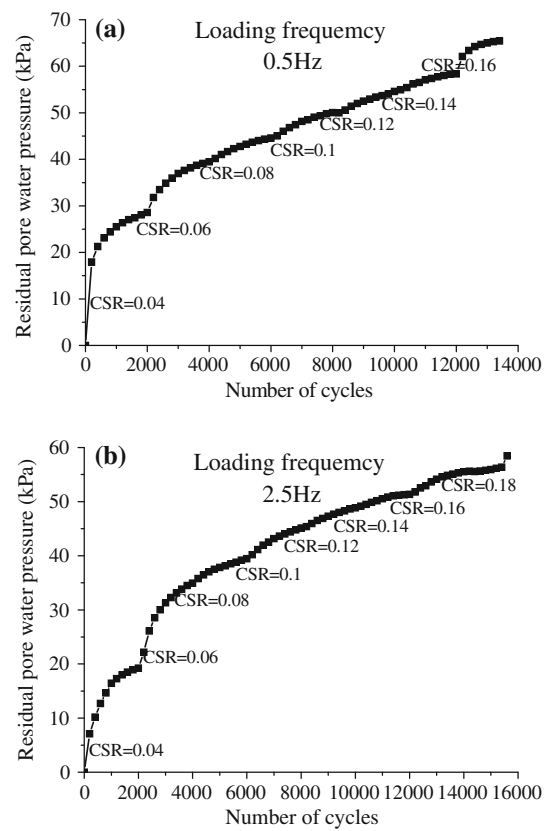


Fig. 10 Residual pore water pressure versus number of cycles with loading frequency

strains are greater under cyclic loading with lower frequency. A significant trend of the curves under the same loading frequency can be detected that the former half segment of the curve is gradually decaying while the latter part turns into accelerated growth, which is also proved the turning point of stability cyclic stress ratio.

Figure 10 describes the variation of residual pore water pressure in the soil samples with loading frequency of 0.5 Hz in Fig. 10a and 2.5 Hz in Fig. 10b. It can be seen that the pore water pressure had a rapid growth initially, and then maintain uniform growth after the growth rate decayed to a stable value. When the stress level was close to the failure cyclic stress ratio, the development of pore water pressure became irregular. In addition, by comparison, the figure implies that it generates larger residual pore water pressure in mucky clay in Shanghai, when subjected to cyclic loading of lower frequency.

Conclusions

In order to solve the engineering geologic problems caused by long-term subway operation loading, the cyclic creep property of mucky clay in Shanghai was investigated

through cyclic triaxial tests under step loading. The results and relevant conclusions of experimental study are summarized and drawn below:

1. Two threshold cyclic stress ratios, the stability cyclic stress ratio and the failure cyclic stress ratio, exist and divide the cyclic creep development into three stages, including the gradual stabilization stage when stress level is below stability CSR, rapid growth stage when stress level is between stability CSR and failure cyclic stress ratio and instantaneous failure stage when stress level is above failure cyclic stress ratio.
2. The cyclic creep process of the mucky clay in Shanghai are composed of two parts, that is, relatively constant recoverable elastic strain and progressively attenuating accumulated plastic strain which obviously detected from the three characteristic creep curves, especially, when the stress level is below failure cyclic stress ratio, there is a linear relation between the recoverable elastic strain and the cyclic stress ratio.
3. It generates greater recoverable elastic strain, accumulated plastic strain and residual pore water pressure in mucky clay in Shanghai, when subjected to the cyclic loading of lower frequency under the same stress level in the frequency section of 0.5–2.5 Hz. The loading frequency has a significant influence on the failure cyclic stress ratio, but not on the stability cyclic stress ratio; and there is larger failure cyclic stress ratio with the increase in loading frequency.

Acknowledgments This investigation is supported by the National Natural Science Foundation of China, Project No.40872178, and Shanghai Leading Academic Discipline Project, Project No.B308, and Kwang-Hua Fund for College of Civil Engineering, Tongji University. The authors are deeply indebted to the three financial supporters.

References

- Andersen KH, Rosenbrand WF, Brown SF et al (1980) Cyclic and static laboratory tests on Drammen clay. *J Geotech Eng Div ASCE* 106:499–529
- Boulanger RW, Idriss IM (2007) Evaluation of cyclic softening in silts and clays. *J Geotech Geoenvir Eng ASCE* 133:641–652. doi:10.1061/1090-0241
- Chai JC, Miura N (2002) Traffic load induced permanent deformation of road on soft subsoil. *J Geotech Geoenvir Eng ASCE* 128:907–916. doi:10.1061/1090-0241
- Guan ZC, Jiang YJ, Tanabashi Y (2009) Rheological parameter estimation for the prediction of long-term deformations in conventional tunneling. *Tunn Undergr Space Technol* 24:250–259
- Hyodo M, Yasuhara K, Hirao K (1992) Prediction of clay behavior in undrained and partially drained cyclic tests. *Soils Found* 32(4):117–127
- Jun J, Chen LZ (2001) One dimensional settlement of soft clay under long-term cyclic loading. *Chin J Geotech Eng* 23(3):366–369
- Miura N, Fujikawa K, Sakai A, Hara K (1995) Field measurement of settlement in Saga airport highway subjected to traffic load. *Tsuchi to Kiso* 43(6):49–51
- Moses GG, Rao SN, Rao PN (2003) Undrained strength behaviour of a cemented marine clay under monotonic and cyclic loading. *Ocean Eng* 30:1765–1789
- Seed HB, Chan CK (1961) Effect of duration of stress application on soil deformation under repeated loading. In: Proceedings 5th International Congress on Soil Mechanics and Foundations 1, Dunod, Pairs, pp 341–345
- Tang YQ, Huang Y, Ye WM et al (2003) Critical dynamic stress ratio and dynamic strain analysis of soil around the tunnel under subway train loading. *Chin J Rock Mech Eng* 22(9):1566–1570
- Tang YQ, Wang YL, Huang Y et al (2004) Dynamic strength and dynamic stress-strain Relation of silt soil under traffic loading[J]. *J Tongji Univ Nat Sci* 32(6):701–704
- Wang R, Liu JH (2000) Monitoring and studying of Shanghai subway's longitudinal deformation during its long time running. *Undergr Eng Tunnel* 4:6–11
- Yilmaz MT, Pekcan O, Bakir BS (2004) Undrained cyclic shear and deformation behavior of silt-clay mixtures of Adapazari. *Turk Soil Dyn Earthq Eng* 24:497–507
- Zhao SK (2005) Study on deformation mechanism of microscopic structure of soft clay under subway loading. Master, Tongji University, Shanghai
- Zhou J, Tu HQ (1996) A model for predicting the cyclic behavior of soft clay. *Rock Soil Mech* 17(1):54–60
- Zhu DF, Huang HW, Yin JH (2005) Cyclic creep behavior of saturated soft clay. *Chin J Geotech Eng* 27(9):1060–1064